analysis of global inundation impacts from sea-level rise, submitted to *Transactions in GIS*, 2006, hereinafter referred to as X. Li et al., submitted manuscript, 2006) as well as the totals for several regions of particular interest (Figure 2). These regions are areas of high population density with economic importance and political influence that, as the results indicate, would sustain marked impacts resulting from sea level rise. The impacts are definitely evident when taking into account population alone, yet the large amount of high-value property for residential, agricultural, and industrial uses is another important impact that needs further investigation. Note specifically the map of inundated areas for 6 meters (Figure 1) in the southeastern United States and the corresponding land area and population affected numbers in Table 1. Equally important in this work is the warning of potential humanitarian crises that are likely to occur as a result of coastal inundation in economically less developed regions with high population densities (e.g., South Asia and Southeast Asia). A hint of such crises, and the accompanying socioeconomic impacts, was felt worldwide in the fallout of the Indian Ocean tsunami of 2004.

Determining an inundation zone for anything less than whole-meter increments is impossible because the vertical resolution of the DEMs used here is whole meters. Yet knowing the land area and population that would be affected by submeter rises in sea level could be illuminating as to more near term impacts of sea level rise. This was accomplished through an interpolation procedure as documented by X. Li et al. (submitted manuscript, 2006).

Several products from this research are now available for use by educators, researchers, policy-makers, and other interested individuals. These products include (1) inundation layers that are viewable in the virtual globe Google Earth©; (2) global and regional static maps of sea level rise (in both PDF and JPEG formats); (3) global and regional map animations of sea level rise (in QuickTime© format); and (4) inundation layers for use in GIS (in ESRI grid format). Each of these products is available for download from the Center for Remote Sensing of Ice Sheets (CReSIS) at http://www.cresis.ku.edu/research/data/sea_level_rise/index.html.

Acknowledgments

The authors wish to thank the following individuals for project assistance: Kalonie Hulbutta of Haskell Indian Nations University, Nathaniel Haas and Johan Feddema of the University of Kansas, and Asif Iqbal and Amber Reynolds of the Kansas Geological Survey. We also appreciate the helpful comments of the anonymous reviewers. This research was supported by the U.S. National Science Foundation under grants ANT-0424589, OPP-0122520, and HRD-0407827.

References

Dobson, J. E., E. A. Bright, P. R. Coleman, R. C. Durfee, and B. A. Worley (2000), LandScan: A global population database for estimating populations at risk, *Photogramm. Eng. Remote Sens., 66*(7), 849–857.

Dyurgerov, M. B., and M. F. Meier. (1997), Year-to-year fluctuations of global mass balance of small glaciers and their contributions to sea-level changes, *Arct. Alp. Res., 29*(4), 392–402.

Hastings, D. A., and P. K. Dunbar (1998), Development and assessment of the Global Land One-km Base Elevation Digital Elevation Model (GLOBE), *Int. Archives Photogramm. Remote Sens., 32*(4), 218–221.

Intergovernmental Panel on Climate Change (2007), *Climate Change 2007, The Physical Scientific Basis: Summary for Policymakers*, 21 pp., Geneva. (Available at http://www.ipcc.ch)

Rignot, E., and P. Kanagaratam (2006), Changes in the velocity structure of the Greenland Ice Sheet, *Science, 311*, 986–990.

NOAA National Geophysical Data Center (2001), 2-minute gridded global relief data (ETOPO2), World Data Cent. for Mar. Geol. and Geophys., Boulder, Colo. (Available at http://www.ngdc.noaa.gov/mgg/fliers/01mgg04.html)

Author Information

Rex J. Rowley, Department of Geography and Center for Remote Sensing of Ice Sheets (CReSIS), University of Kansas, Lawrence; E-mail: rjrowls@ku.edu; John C. Kostelnick, College of Mathematics and Natural Sciences, Haskell Indian Nations University, Lawrence, Kans.; David Braaten and Xingong Li, Department of Geography and CReSIS, University of Kansas, Lawrence; and Joshua Meisel, College of Mathematics and Natural Sciences, Haskell Indian Nations University, Lawrence, Kans., and CReSIS, University of Kansas, Lawrence.

How Nature Foiled the 2006 Hurricane Forecasts

PAGES 105–107

The 2006 hurricane season proved again that predicting Mother Nature is a very precarious undertaking.

At the beginning of the season, all signs indicated that it would be more active than average: Sea surface temperature (SST) was above normal, vertical wind shear was low, and sea level pressure was reduced over the tropical Atlantic. Many forecasters believed that these features foreshadowed a continuation of the trend of nine preceding years of above-normal hurricane seasons. Given the recent warming tendency in the Atlantic and the prevailing favorable preseason conditions, there was no wonder that even by August 2006, forecasters were still calling for an above-normal frequency of tropical storms and hurricanes.

By W. K. M. Lau and K.-M. Kim

In the end, however, the 2006 hurricane season was near normal with four tropical storms and five hurricanes, but decidedly lackadaisical compared with the record numbers of 12 tropical storms and 15 hurricanes in 2005. Most impressive was the fact that while five hurricanes, including Katrina, made landfall in the United States in 2005, no hurricane even came close to threatening the U.S. Gulf coast or eastern seaboard in 2006.

How did nature foil all attempts to forecast the 2006 hurricane season? Undoubtedly, this question, together with others, will be addressed by many studies to come. In this article we present new insights derived from preliminary analysis using satellite data, with the intention of stimulating further studies. Data used for this study include SST, rainfall, cloud top temperature, water vapor from the Tropical Rainfall Measuring Mission (TRMM), and aerosol index (AI) from the Ozone Monitoring Instrument (OMI) on the satellite Aura.

Tropical Storm and Hurricane Tracks

During July-August-September (JAS) 2005, there were nine distinct tropical storm and hurricane tracks over the warm pool (SST > 28°C) in the western Atlantic and Caribbean (WAC), and the Gulf of Mexico (Figure 1a). Five hurricanes made landfall over the Gulf coast and the eastern seaboard of the United States. In 2006, no hurricanes were found over the WAC and the Gulf region. Four distinct tropical storm/hurricane tracks were found at the northeastern edge of the warm pool far away from the eastern coast of the United States (Figure 1b). Only two tropical storms formed over the WAC and the eastern seaboard of the United States, but they never developed into hurricanes.

A closer look at the full hurricane season (July through November) indicates that in 2005, the tropical storm and hurricane tracks can be classified into two groups. For group 1, tropical storms were generated within 10°–15°N over the eastern Atlantic, and intensified with a clockwise track off the northwestern edge of the warm pool, east of 65°W. For group 2, tropical storms were generated and subsequently intensified to hurricane strength over the very warm water (>29°C) of the WAC and the Gulf of Mexico. Long-term climatology analysis of the past 30 hurricane seasons shows that group 1 occurs more often in the early season (June–August), while group 2 is more frequent in the late season (September–November). In 2006, even though the water over the Gulf of Mexico remained very warm (SST > 29ºC), the WAC was substantially cooler, and there were no group 2 tropical storms or hurricanes, contrasting with 2005 when group 2 tropical storms and hurricanes were prevalent.

Table 1. Correlation of Barbados Dust Index and Niño-3 Sea Surface Temperature With Three Sets of Storm Measures: FOC, ACE, and SI[a]

JASON 1980–2003		50º–20ºW, 5º–15ºN Genesis Region (GNR)		70º–40ºW, 15º–30ºN Intensification Region (ITR)	
		Dust	Niño-3 SST	Dust	Niño-3 SST
Frequency of occurrence (FOC)[b]	TS	-0.376	-0.383	-0.012	-0.157
	HC	-0.371	**-0.403**	**-0.477**	-0.364
	ALL	**-0.404**	**-0.418**	-0.292	-0.300
Accumulated cyclone energy (ACE) index[c]	TS	**-0.502**	**-0.402**	-0.156	-0.272
	HC	-0.363	**-0.421**	**-0.465**	-0.326
	ALL	**-0.453**	**-0.455**	**-0.441**	-0.326
Storm intensity (SI)[d]	TS	**-0.659**	0.130	-0.262	-0.255
	HC	0.097	**-0.511**	-0.244	-0.055
	ALL	**-0.501**	-0.350	**-0.506**	-0.395

[a]Correlations exceeding the 5% confidence level are shown in bold. All correlations are computed separately for three storm categories: TS, tropical storm only; HC, hurricane only; and ALL, tropical storm or hurricane.

[b]FOC is defined as the total number of days from July through November (JASON) in which a given storm category is found within the region.

[c]ACE is the square of the maximum sustained wind speed of storm at every 6 hours.

[d]SI is defined as the ACE divided by FOC.

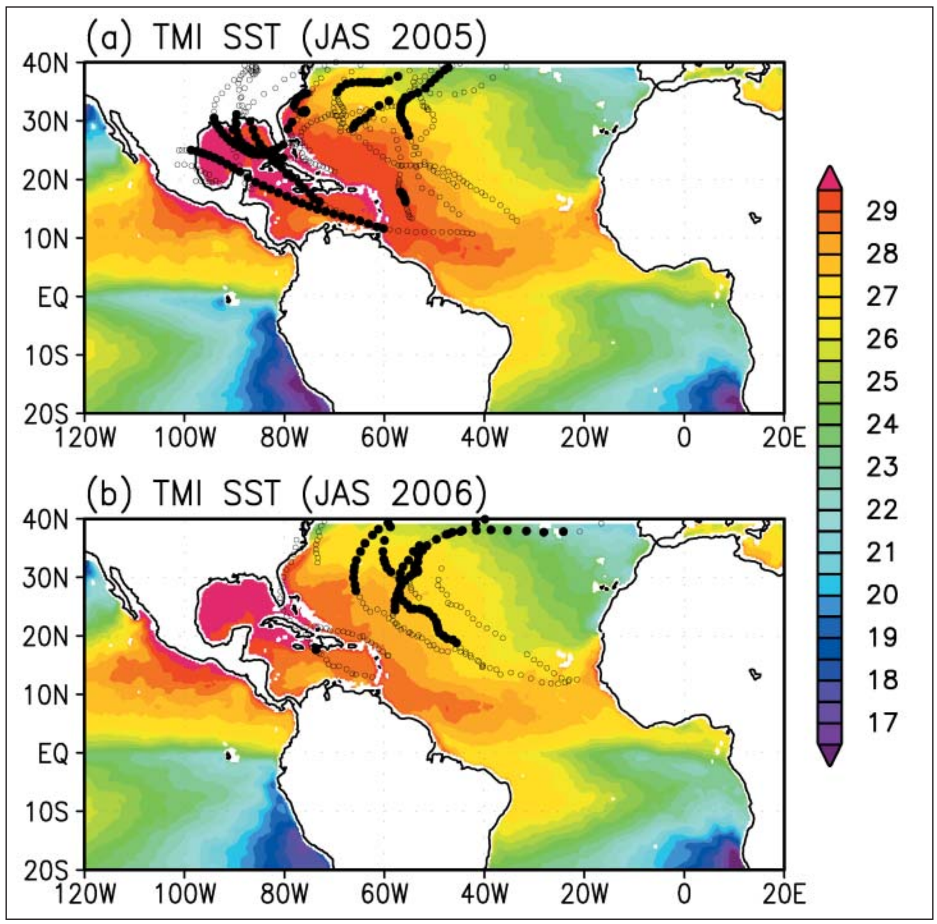

Fig. 1. Tropical storm tracks (open circles) and hurricane tracks (solid circles) superimposed on seasonal mean (July-August-September, JAS) fields of TRMM Microwave Instrument (TMI) sea surface temperature (SST) (ºC) for (a) 2005 and (b) 2006.

SST, Dust, Precipitation, and Cloud Anomalies

The cooling of the Atlantic in 2006 relative to 2005 was widespread, covering most of the subtropical and equatorial North Atlantic, with the strongest signal (~0.6º–0.8ºC) over the WAC (Figure 2a). This cooling was spectacular in its magnitude and extent, particularly considering that the Atlantic Ocean was supposed to be in the midst of a long-term warming trend. Also noted was substantial warming in the eastern equatorial Pacific and the Gulf of Guinea. The former can be identified with the signals of a moderate El Niño, which was emerging in JAS 2006.

Concomitant with the cooling of the North Atlantic was a substantial increase in atmospheric dust loading in 2006, covering nearly all the northern tropical and subtropical Atlantic and western Africa (Figure 2b), with the oceanic maximum over the WAC, where the negative SST anomaly was most pronounced. A major reduction in aerosol loading, most likely associated with reduced biomass burning, was also found over the Amazon and off the coast of western South Africa between 0º and 20ºS.

With the exception of the eastern Pacific, the dust anomaly pattern corresponds well, but in an inverse relationship with the SST pattern, with the areas of negative (positive) SST anomalies having positive (negative) dust anomalies overhead. This suggests that the extensive cooling over the subtropical North Atlantic may be related to the shielding of solar radiation (the so-called solar dimming effect) by dust. Examination of the anomaly pattern of surface wind speed from the TRMM Microwave Imager indicated that the surface wind speed was also significantly higher over the negative SST anomalies in the WAC. An increase in surface wind speed could enhance surface evaporation and upper ocean mixing, both of which would have cooled the ocean, further contributing to the extensive negative SST anomaly.

In 2006 the JAS mean rainfall over the eastern Atlantic and West Africa along 10ºN was generally higher than in 2005, while that over the WAC and the Gulf of Mexico was deficient compared with 2005 (Figure 2c). Since climatologically tropical storm- and hurricane-related rainfall contributes not more than 5% of the total seasonal rain over the entire North Atlantic [*Rogers et al.*, 2001], the reduction in total seasonal rain over the western North Atlantic and Gulf region cannot be due to tropical storms and hurricanes. Rather, the dipole-like rainfall anomaly signaled a shift in circulation regime with a more convectively active eastern Atlantic Intertropical Convergence Zone (a belt of low air pressure near the equator) and an enhanced West African monsoon, coupled with a convectively less active western Atlantic.

This picture is supported by the difference map of TRMM/Visible Infrared Scanner (VIRS) brightness temperature (T_b; Figure 2d), with the eastern Atlantic and West Africa region dominated by negative signals (cold cloud top, increased deep convection) and the WAC and the Gulf region with positive signals (low cloud top, reduced deep convection). In concert with the rainfall and the T_b

patterns, the TRMM total water vapor also indicates a moister eastern Atlantic and a drier western Atlantic in 2006. The patterns of SST, rainfall, and T_b are also consistent with anomalous large-scale rising of air over the eastern Atlantic and sinking over the western Atlantic found in reanalysis data from the U.S. National Centers for Environmental Prediction. This is indicative of an anomalous (in the sense of the difference between 2006 and 2005) Walker-type circulation connecting the atmospheres of the two regions. The large-scale subsidence over the WAC and the Gulf of Mexico could have further suppressed deep convection and tropical storm and hurricane formation over those regions.

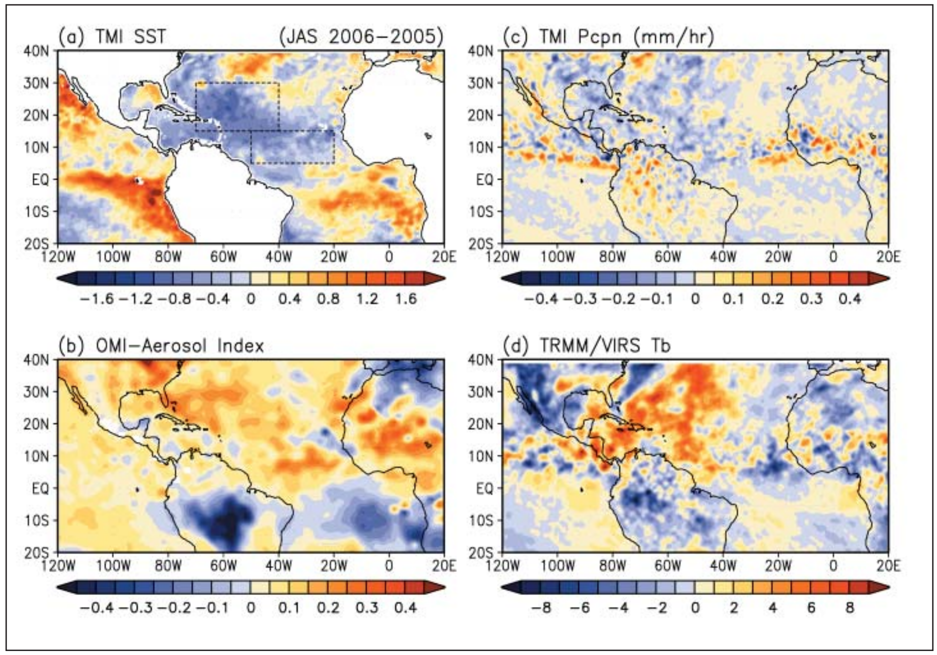

Fig. 2. Maps show difference between JAS 2006 and 2005 (2006 minus 2005) of (a) SST (°C), (b) OMI/AI (units are nondimensional), (c) TMI rainfall (millimeters per hour), and (d) Visible Infrared Scanner cloud top temperature (T_b, °C).

Covariability of North Atlantic SST and Dust

Figure 3 shows the time series of daily SST and OMI/AI for 2005 and 2006 over a region in the WAC, marked by the large rectangle in Figure 2a. This region saw the largest negative SST anomaly in 2006. It also coincides with the geographic location where group 2 hurricanes are most likely to spawn climatologically. From the start of the seasonal warming in mid-March, the 2006 SST did not rise as fast compared with 2005, producing a relative initial cooling of 0.2°–0.5°C that lasted through mid-May. The most pronounced SST cooling began in mid-June 2006, reaching a maximum (>1°C) in late June and mid-July, until the end of September after which the SST returned to the 2005 level (Figure 3a).

The SST cooling appeared to be closely related to the variation of Sahara dust over the region. Overall, the dust loading in 2006 was higher than in 2005 (Figure 3b). An initial anomalous increase in dust began in late February and early March 2006, about 2–3 weeks prior to the initial SST cooling, and lasted until late May. Most striking was a major increase in dust loading at the beginning of June, 2 weeks prior to the major SST cooling. This major dust episode lasted for about a month, until the end of June. The two episodes of SST cooling in the region appeared to be phase-locked to increased dust loading in the region, with a delay of about 2–3 weeks. Considering the episodic nature of the 2006 Atlantic cooling, particularly the abruptness of the SST drop at the start of the hurricane season, the 2006 Atlantic cooling was clearly not part of a long-term trend but possibly the result of a basin-wide coupled ocean-atmosphere interaction spurred by a dust-induced solar dimming effect.

Historical Effects of Dust and El Niño

Table 1 shows the correlation coefficients (cc) of the dust and Niño-3 SST (monthly mean averaged over the region 5°N–5°S, 150°–90°W) with three sets of storm measures (frequency of occurrence, FOC; accumulated cyclone energy, ACE; and storm intensity, SI) for three storm categories (HC, hurricane only; TS, tropical storm only; and ALL, hurricane or tropical storm). Detailed definitions are provided in the Table 1 footnotes. For dust, we use the Barbados record, which is the only multidecadal dust record that exists and has been shown to be highly correlated with the outbreak of dust from North Africa over the North Atlantic [*Prospero and Lamb*, 2002]. All correlations are computed for two domains, the genesis region (GNR; 50°–20°W, 5°–15°N) and the intensification region (ITR; 70°–40°W, 15°–30°N), for the period 1980–2003.

As shown in Table 1, in the GNR both dust and El Niño have significant influences on tropical storms and hurricanes. Dust has a stronger influence on tropical storms than on hurricanes in all three measures, with the strongest signal in tropical storm intensity (cc = 0.659). In contrast, El Niño has a stronger influence on hurricanes relative to tropical storms, again with strongest influence in intensity (cc = 0.511). Taken over all categories and measures, El Niño has a stronger influence (more cases of significant correlations) in the GNR compared with dust, most likely through an increase in the vertical wind shear [*Goldenberg and Shapiro*, 1996], which inhibits cyclogenesis over the GNR. Compared with the GNR, dust influences in the ITR remain strong, showing significant negative correlations for hurricane frequency (cc = –0.477), hurricane strength (cc = –0.465), and ALL intensity (cc = –0.506). In contrast, the influence of El Niño is substantially diminished in the ITR, showing no significant correlations on any measures or categories.

In conclusion, our results suggest that the increased atmospheric loading of Saharan dust over the North Atlantic during the 2006 hurricane season might have been instrumental in initiating a climate regime shift in the coupled ocean-atmosphere system of the tropical and subtropical Atlantic. Associated with the shift were rapid basin-scale cooling in the North Atlantic and suppressed tropical storm and hurricane activity in the western Atlantic and the Caribbean. Historical data also support this thesis, indicating that Saharan dust may have a stronger influence than El Niño on hurricane statistics in the subtropical western Atlantic/Caribbean region, while El Niño influence may be stronger in the tropical eastern Atlantic.

Finally, we should point out that the possible roles of Saharan dust on tropical storms and hurricanes in cooling SST described here are climatic impacts, which are distinct from the dynamic effects of the Saharan air layer (SAL) in suppressing cyclogenesis and individual tropical storm and hurricane development [*Dunion and Veldon*, 2004]. How SAL modulated individual tropical storms or hurricanes in 2005 and 2006, and how the modulations are affected by large-scale circulation and Atlantic SST changes, are clearly important subjects for further studies.

Acknowledgments

This work was supported jointly by the NASA Precipitation Measuring Mission, the NASA Africa Monsoon Multiscale Analysis, and the Interdisciplinary Investigation Program of the Earth Science Division, NASA Headquarters. J. Prospero kindly provided the Barbados dust data for this study.

References

Dunion, J. P., and C. S. Velden (2004), The impact of the Saharan air layer on Atlantic tropical cyclone activity, *Bull. Am. Meteorol. Soc.*, *85*, 353–365.

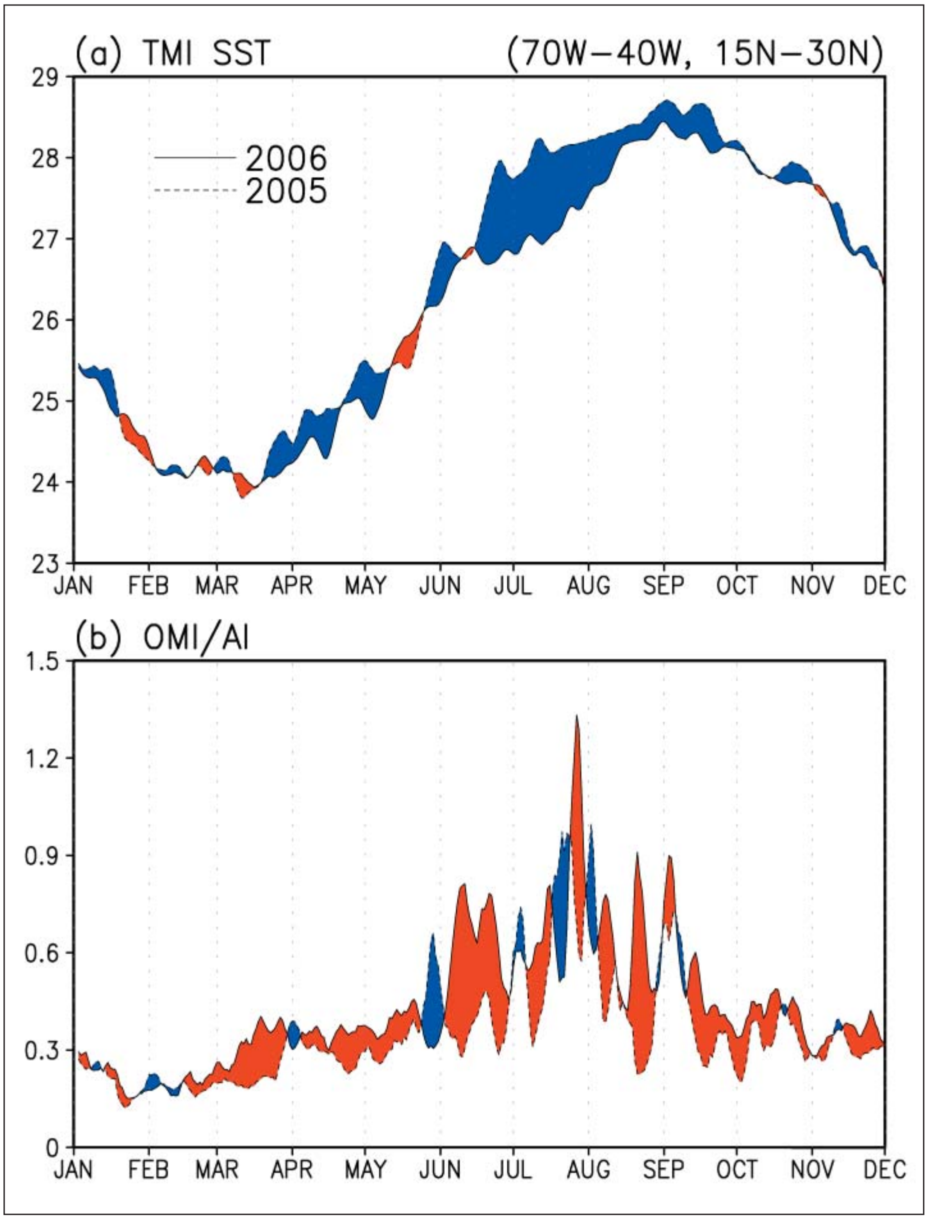

Fig. 3. Time series showing daily (smoothed by a 5-day running mean) variation of (a) SST and (b) OMI/AI, in the western Atlantic and Caribbean (WAC) region (70°–40°W, 15°–30°N) in 2005 and 2006. Blue (red) color indicates negative (positive) anomaly in 2006 relative to 2005.

Goldenberg, S. B., and L. J. Shapiro (1996), Physical mechanisms for the association of El Niño and West African rainfall with Atlantic major hurricane activity, *J. Clim.*, *9*, 1169–1187.

Prospero, J. M., and P. J. Lamb (2003), African droughts and dust transport to the Caribbean: Climate change implications, *Science*, *302*, 1024–1027.

Rogers, E. B., R. F. Adler, and H. F. Pierce (2001), Contribution of tropical cyclones to the North Atlantic rainfall climatology as observed from satellites, *J. Appl. Meteorol.*, *40*, 1785–1800.

Author Information

William K. M. Lau, Laboratory for Atmospheres, NASA Goddard Space Flight Center, Greenbelt, Md.; E-mail: William.k.lau@nasa.gov; and Kyu-Myong Kim, Goddard Earth Sciences and Technology Center, University of Maryland Baltimore County, Baltimore.